Institute of Paper Science and Technology
Atlanta, Georgia

IPST Technical Paper Series Number 848

The Mechanics of Sorption-Induced Transients in the Loss Tangent

D.W. Coffin and C.C. Habeger

April 2000

Submitted to
Journal of Pulp and Paper Science

INSTITUTE OF PAPER SCIENCE AND TECHNOLOGY
PURPOSE AND MISSIONS

The Institute of Paper Science and Technology is an independent graduate school, research organization, and information center for science and technology mainly concerned with manufacture and uses of pulp, paper, paperboard, and other forest products and byproducts. Established in 1929 as the Institute of Paper Chemistry, the Institute provides research and information services to the wood, fiber, and allied industries in a unique partnership between education and business. The Institute is supported by 52 North American companies. The purpose of the Institute is fulfilled through four missions, which are:

- to provide multidisciplinary graduate education to students who advance the science and technology of the industry and who rise into leadership positions within the industry;
- to conduct and foster research that creates knowledge to satisfy the technological needs of the industry;
- to provide the information, expertise, and interactive learning that enables customers to improve job knowledge and business performance;
- to aggressively seek out technological opportunities and facilitate the transfer and implementation of those technologies in collaboration with industry partners.

ACCREDITATION

The Institute of Paper Science and Technology is accredited by the Commission on Colleges of the Southern Association of Colleges and Schools to award the Master of Science and Doctor of Philosophy degrees.

NOTICE AND DISCLAIMER

The Mechanics of Sorption-Induced Transients in the Loss Tangent

Douglas W. Coffin and Charles C. Habeger

Institute of Paper Science and Technology
500 10th Street N.W., Atlanta, GA30318

ABSTRACT

We demonstrate mathematically that hygroexpansive materials displaying nonlinear viscoelastic behavior can have larger loss tangents during and immediately after moisture changes than they do at equilibrium. Our analyses reveal that these sorption-induced transients can result directly from stress gradients created by moisture changes. Further calculations show that artificial transients can arise from improper data analysis. Together, these observations support the contention that part of the loss tangent transient phenomenon is real but that much of the large transient excursions reported in the literature are artifacts of the test methods.

BACKGROUND

It is frequently claimed that loss tangents, as determined by small-strain sinusoidal loading experiments, are larger during and immediately after sorption than they would have been at the same equilibrium moisture content. Moisture-induced artifacts that could account for at least part of the disagreement are rarely acknowledged or considered. Nevertheless, loss tangent excesses are consistently observed long after sorption is complete and these measurement artifacts have ceased to be operative.

For cellophane and paper in changing moisture and ammonia atmospheres, Kubát and Lindbergson [1,2] calculated loss tangents from the amplitude changes of a freely oscillating torsion pendulum. They registered large (factor of 2 and more) damping transients upon absorption and desorption. They encountered a disconcertingly large unexplained longitudinal load influence on loss tangent and torsional stiffness [1] that troubles us when interpreting their transient results. For the strip dimensions that they employed, the stiffness parameter governing the oscillation dynamics of a homogeneous sheet is $G_{23}bd^3/3L$, where G_{23} is the complex in-plane shear modulus, b is the sheet width, and d is the sheet thickness. Irrespective of loss processes, the amplitude of the freely oscillating torsion pendulum will change during sorption as $G_{23}bd^3/3L$ changes. Neglecting this effect, they took the loss tangent as being directly proportional to the log decrement of the oscillation amplitude. They also did not consider temperature changes due to sorption and through-sheet stiffness distribution effects. Nevertheless, the loss tangents maintained their depressions long after the sorption events were complete and after these criticisms had relevance. De Ruvo et al.

[3] report similar results from what appear to be torsion pendulum experiments on single wood fibers.

Commercial dynamic mechanical thermal analyzers (DMTA's) are intended to measure the dynamic stiffnesses and loss coefficients of polymers under slowly changing temperature conditions. Nonetheless, they have been used to monitor sorption transient effects. Stiffness coefficients are reported directly from unspecified internal calculations, which assume that dimensional changes, stiffness changes, and stiffness redistribution within a cycle are negligible. When the instrument is confronted with a rapidly sorbing material, the meanings of the standard outputs (especially the loss coefficients) are unclear. As the frequency increases, less material change occurs during each measurement cycle and artifacts from material inconstancy decrease. Padanyi [4] used a DMTA manufactured by Polymer Laboratories to study samples of kraft linerboard bending. Large transient increases in loss tangent and decreases in bending stiffness were detected. The influences of heat of sorption, moment of inertia changes due to swelling, and through-sheet stiffness gradients were not considered. The drastic decreases of transients observed as the frequency increased are consistent with a measurement artifact explanation. On the other hand, the persistence of the loss tangent excesses long after sorption was complete supports the argument that the effect is partly real.

Salmén and Fellers [5] performed dynamic tensile modulus measurements on paper and Nylon 6,6 fibers during sorption on a Perkin Elmer DMA7e. They report absorption and desorption loss tangent transients that decrease as frequency goes from 0.2 to 11 Hz. In paper, they saw an absorption-induced undershoot in the real part of the modulus, which one might attribute to the heat of sorption. They argue that their loss tangent transient observations are a consequence of the non-loop-closure artifact caused by the hygroexpansion occurring in one cycle. Tensile DMTA loss and modulus transients are also reported by Jackson and Parker [6] and Denis and Parker [7] in wood fibers and in kraft papers. Berger [8] made cyclic stiffness measurements on paper in an Instron tensile instrument during sorption. Even after making a correction for the non-loop-closure effect, loss transients remained.

Berger and Habeger [9] investigated the influence of changing RH on in-plane ultrasonic stiffnesses. Ultrasonic stiffnesses were measured at such high frequencies (about 80 KHz) that material changes during a test cycle were inconsequential. They found that, after proper corrections were made for the temperature changes caused by sorption, the real part of the stiffness was the same during sorption as it was at the same equilibrium moisture content. No desorption loss tangent transient was observed. There was a small overshoot in the absorption loss tangent, but this was ascribed to an absorption-induced temperature rise.

Possibly the cleanest experiments that demonstrate that paper is more compliant after moisture changes are the creep tests of Padanyi [10]. He clearly shows that, even after moisture equilibrium is reached, creep rates decrease as the time lapse between moisture change and load application increases. These creep experiments have a much longer time frame than dynamic stiffness tests, and they exhibit a larger, longer-lasting effect. Padanyi's findings further sway us toward the opinion that paper, as well as other swelling polymers, is more compliant in long-time experiments after a sorption event.

From the past work, we draw the conclusion that there are true moisture-transient loss tangent effects that become less prominent as the time frame of the experiment is decreased. During sorption and at low frequencies, a good portion of the excursion may well be a result of measurement artifacts. However, the general observations at low frequency of compliance excesses after sorption are hard evidence for a real phenomenon.

Previously, we proposed that accelerated creep and physical aging are manifestations of sorption-induced stress gradients and nonlinear creep compliance [11]. We argued that sorption can create substantial stress gradients in hygroexpansive materials. This happens either as result of moisture gradients established during sorption or because the material responds heterogeneously to moisture. For many materials, compliance increases more than linearly with load. This nonlinear behavior is especially evident in long-time responses, such as creep, which require long-range polymer backbone motions. When stress gradients are established, the extra compliance in regions of high stress results in a more overall compliant material. After sorption, these residual stresses decay through viscoelastic relaxation, and the material slowly returns to its stiffer equilibrium state. It is already established that paper dynamic modulus measurements depend on the applied cyclic strain amplitude [12,13]. Loss tangents increase and storage moduli decrease with strain amplitude. Furthermore, the sensitivity of this dependence is greater at lower frequency [13]. In the following, we show that materials experiencing this type of nonlinear, viscoelastic behavior are prone to exhibit transient effects if stress gradients are present.

We maintain [11] that for paper both heterogeneity and moisture gradients contribute to the stress gradients that generate accelerated creep. We suspect that the moisture gradient portion makes the larger contribution for paper and is the predominant cause of accelerated creep in cellophane and synthetic fibers. A gradient in moisture change creates a gradient in the potential for hygroexpansion that in turn manifests as a stress gradient. We envision that the pertinent heterogeneity is on a fiber-to-fiber level. Fiber hygroexpansivity is much greater in the radial direction than along the axial direction. When fibers with different axial alignments are bonded together in a sheet, their hygroexpansions are not compatible, and stresses develop during moisture changes. Presumably, these two actions, which create the stress gradients leading to accelerated creep, also produce stress gradients that generate loss tangent transients. In the following we make no attempt to model the processes that we suspect control the response of paper. Instead, we provide an easily visualized model of a laminate that clearly demonstrates that sorption-induced stress gradients can cause loss tangent transients. It convinces us that the other, more likely, means of producing stress gradients will also create transients. We intend only to convince the reader that the process is plausible in general. Because it is mathematically expeditious, we employ simple constitutive equations and handle only the case in which the stress gradients are generated by heterogeneous hygroexpansion. We insist, however, that the same processes prevail regardless of the complexity of the constitutive behavior and of the mechanism that generates sorption-induced stress gradients.

ANALYTICAL DEVELOPMENT

Governing Equations

Consider a hygroexpansive and nonlinear viscoelastic material. Assume the total strain is the sum of linear-elastic, linear viscous, power-law-viscous, and linear-hygroexpansive strains. That is, the strain rate, $\partial\varepsilon/\partial t$, at any point in the material can be written as

$$\frac{\partial \varepsilon}{\partial t} = \frac{\partial(\sigma / E)}{\partial t} + \frac{1}{\eta}\sigma + \lambda\sigma^n + \frac{\partial(\beta\Delta m)}{\partial t} \tag{1}$$

In Eq. (1), η is the viscosity of linear component of the viscous response, λ and the odd integer, n, represent nonlinear viscous parameters, E is the elastic modulus, β is the hygroexpansion, Δm is the change in moisture, and σ is the stress.

In general, the mechanical properties, the stress, and the strain are functions of time and position in the material. We consider a material in a state of uniaxial loading and uniform strain. Therefore, the strain is a function of time only, while the stress can be a function of position and time. To further simplify the formulation, we choose a symmetric three-ply sheet. Each outer ply has one half the thickness of the middle ply. We assume that all properties of the plies are equal except the hygroexpansion. Furthermore, we require the moisture to be evenly distributed at all times. Under these assumptions, the deformation of the laminate is governed by Eqs. (2-5).

$$\frac{d\varepsilon}{dt} = \frac{1}{E}\frac{\partial\sigma_1}{\partial t} + \frac{1}{\eta}\sigma_1 + \lambda\sigma_1{}^n + \beta_1\frac{\partial m}{\partial t} \tag{2}$$

$$\frac{d\varepsilon}{dt} = \frac{1}{E}\frac{\partial\sigma_2}{\partial t} + \frac{1}{\eta}\sigma_2 + \lambda\sigma_2{}^n + \beta_2\frac{\partial m}{\partial t} \tag{3}$$

$$\sigma_1 + \sigma_2 = 2\sigma_{avg} \tag{4}$$

$$\varepsilon(0) = \frac{\sigma_{avg}(0)}{E},\ \sigma_1(0) = \sigma_{avg}(0), \sigma_2(0) = \sigma_{avg}(0) \tag{5}$$

Above, the subscript 1 denotes the outer plies, the subscript 2 denotes the inner ply, and σ_{avg} is the applied force at any time divided by the total cross-sectional area of the sheet.

Solution for Case of Constant Moisture

We subject the laminate to constant load and a small sinusoidal test load at a constant moisture content, $m(t)$=constant,

$$\sigma_{avg}(t) = \sigma_0 + \Delta\sigma \sin(\omega t) \tag{6}$$

For this case, the stresses are equal, $\sigma_1 = \sigma_2 = \sigma_{avg}$, and the strain, obtained by direct integration of Eq. (2) with the initial condition, Eq. (5), is

$$\begin{aligned}\varepsilon(t) = \frac{\sigma_0}{E} + C + \left[\frac{\sigma_0}{\eta} + \lambda\sigma_0^{\ n}\left[1 + F_1(\frac{\Delta\sigma}{\sigma_0})\right]\right]t \\ + \frac{\Delta\sigma}{E}\sin(\omega t) - \Delta\sigma\left[\frac{1}{\eta\omega} + \frac{n\lambda\sigma_0^{\ n-1}}{\omega}\left[1 + F_2(\frac{\Delta\sigma}{\sigma_0}, t)\right]\right]\cos(\omega t)\end{aligned} \tag{7}$$

where

$$F_1(\frac{\Delta\sigma}{\sigma_0}) = \sum_{j=1}^{(n-1)/2} \frac{n!}{2^{2j}(n-2j)!\, j!^2}\left(\frac{\Delta\sigma}{\sigma_0}\right)^{2j},$$

$$F_2(\frac{\Delta\sigma}{\sigma_0}, t) = \sum_{j=2}^{n} \frac{(n-1)!}{(n-j)!\, j!}\left(\frac{\Delta\sigma}{\sigma_0}\right)^{j-1} \begin{cases} \displaystyle\sum_{i=1}^{(j+1)/2} \frac{(j+1-2i)!}{j!}\left[\frac{2^{i-1}((j-1)/2)!}{((j+1-2i)/2)!}\right]^2 sin^{j+1-2i}(\omega t) \text{ if } j \text{ is odd} \\ \displaystyle\sum_{i=1}^{j/2} \frac{j!}{(j/2)!}\left[\frac{((j/2)-i)!}{2^i(j-2i+1)!}\right]^2 sin^{j+1-2i}(\omega t) \text{ if } j \text{ is even} \end{cases}$$

and

$$C = \Delta\sigma\left[\frac{1}{\eta\omega} + \frac{n\lambda\sigma_0^{\ n-1}}{\omega}\left[1 + F_2(\frac{\Delta\sigma}{\sigma_0}, 0)\right]\right]$$

The first two terms in Eq. (7), $\sigma_0/E + C$, are integration constants added to insure that the initial strain is the instantaneous elastic response, σ_0/E. The third term is the overall creep response, which is a linear function of time and a nonlinear function of load. The term, $F_1(\Delta\sigma/\sigma_0)$, represents the increase in the creep rate due to the sinusoidal load. For $n=1$, the material behavior is linear, $F_1(\Delta\sigma/\sigma_0) = 0$, and the cyclic load creates no excess creep. When $n>1$, cyclic loading leads to excess creep above the creep created by the mean load, σ_0. We argue that this type of excess creep is the source of accelerated creep in which load cycling is created by humidity changes [11].

The fourth and fifth terms of Eq. (7), which represent the dynamic response, are the main concerns of this article. The fourth term is the elastic part of sinusoidal response, which is in phase with the stress. The fifth term is the out-of-phase, viscous response. Notice that the elastic response is at the same frequency as the cyclic stress, whereas the viscous term includes harmonic terms through $F_2(\Delta\sigma/\sigma_0, t)$. Like $F_1(\Delta\sigma/\sigma_0)$, $F_2(\Delta\sigma/\sigma_0, t)$ is a direct consequence of material nonlinearity.

The loss tangent is defined in the limit as the amplitude of the sinusoidal load approaches zero. For the case in which the amplitude of the cyclic load is small compared to the applied force, the higher order terms in $\Delta\sigma/\sigma_0$ are negligible, $F_2(\Delta\sigma/\sigma_0, t) \approx 0$, and Eq. (7) becomes

$$\varepsilon_{dyn}(t) = \frac{\Delta\sigma}{E\, cos(\delta)} sin(\omega t - \delta) \tag{8}$$

where

$$\tan(\delta) = \frac{E}{\eta\omega} + \frac{n\lambda\sigma_0^{\,n-1}E}{\omega} \tag{9}$$

The total loss tangent is the sum of the loss tangents of the linear and nonlinear viscous components. From Eq. (9), we see that the magnitude of the loss tangent increases with both the magnitude of the applied constant load and the exponent n. In our opinion, this dependence of loss tangent upon load is the source of moisture-induced loss tangent transients.

Solution for Case of Sorption

Now let moisture vary with time. Since the hygroexpansions of the inner and outer plies are not equal, a sorption-induced stress will be created in each ply. These sorption-induced stresses are equal in magnitude but opposite in sign. They add to the stress resulting from the external load, Eq. (6), and influence the loss tangent.

To calculate loss tangent, we are interested only in the case where $\Delta\sigma$ is small compared to any applied or sorption-induced stresses. Therefore, a first-order linear perturbation of the solution with respect to $\Delta\sigma$ will yield the solution for the loss tangent. In other words, we assume that $\Delta\sigma$ is very small and that the solutions to Eqs. (2-5) are of the form

$$\begin{aligned}
\sigma_1(t) &= \hat{\sigma}_1(t) + \Delta\sigma\left[A_1 \sin(\omega t) + B_1 \cos(\omega t)\right] \\
\sigma_2(t) &= \hat{\sigma}_2(t) + \Delta\sigma\left[A_2 \sin(\omega t) + B_2 \cos(\omega t)\right] \\
\varepsilon(t) &= \hat{\varepsilon}(t) + \frac{\Delta\sigma}{E}\left[A_3 \sin(\omega t) + B_3 \cos(\omega t)\right]
\end{aligned} \tag{10}$$

Substituting these expressions into Eqs. (2-5) and retaining only terms up to first order in $\Delta\sigma$ gives the following equations:

$$\frac{d\hat{\varepsilon}}{dt} = \frac{1}{E}\frac{\partial\hat{\sigma}_1}{\partial t} + \frac{1}{\eta}\hat{\sigma}_1 + \lambda\hat{\sigma}_1^{\,n} + \beta_1\frac{\partial m}{\partial t} \tag{11}$$

$$\frac{d\hat{\varepsilon}}{dt} = \frac{1}{E}\frac{\partial\hat{\sigma}_2}{\partial t} + \frac{1}{\eta}\hat{\sigma}_2 + \lambda\hat{\sigma}_2^{\,n} + \beta_2\frac{\partial m}{\partial t} \tag{12}$$

$$\hat{\sigma}_1 + \hat{\sigma}_2 = 2\sigma_0 \tag{13}$$

$$\hat{\varepsilon}(0) = \frac{\sigma_0}{E},\ \hat{\sigma}_1(0) = \hat{\sigma}_{avg}(0), \hat{\sigma}_2(0) = \hat{\sigma}_{avg}(0) \tag{14}$$

and

$$A_3 \cos(\omega t) - B_3 \sin(\omega t) = \left[A_1 + \tan(\delta_1)B_1\right]\cos(\omega t) - \left[B_1 - \tan(\delta_1)A_1\right]\sin(\omega t) \tag{15}$$

$$A_3 \cos(\omega t) - B_3 \sin(\omega t) = \left[A_2 + \tan(\delta_2)B_2\right]\cos(\omega t) - \left[B_2 - \tan(\delta_2)A_2\right]\sin(\omega t) \tag{16}$$

$$(A_1 + A_2)\sin(\omega t) + (B_1 + B_2)\cos(\omega t) = 2\sin(\omega t) \tag{17}$$

where

$$\tan(\delta_1) = \frac{E}{\eta\omega} + n\frac{\lambda E}{\omega}\hat{\sigma}_1^{\,n-1} \text{ and } \tan(\delta_2) = \frac{E}{\eta\omega} + n\frac{\lambda E}{\omega}\hat{\sigma}_2^{\,n-1} \tag{18}$$

are the loss tangents of each ply. A comparison of Eqs. (11-14) with Eqs. (2-5) reveals that $\hat{\varepsilon}$ is the strain and that $\hat{\sigma}_1$ and $\hat{\sigma}_2$ are the ply stresses resulting from the applied load and change in moisture. Equations (15-18) govern the linear dynamic response of the material due to the applied cyclic load.

To determine the influence of a specific sorption event on the loss tangent, we impose a moisture history and numerically solve Eqs. (11-14) for $\hat{\sigma}_1$ and $\hat{\sigma}_2$ with no sinusoidal load applied. Then, we insert these values into Eqs. (15-17) and solve the six resulting algebraic equations for the coefficients, A_i and B_i. The loss tangent as a function of the sorption-induced stresses through Eq. (18) is

$$\tan(\delta) = -\frac{B_3}{A_3} = \left[\tan(\delta_1) + \tan(\delta_2)\right]\frac{1+\tan(\delta_1)\tan(\delta_2)}{2+\tan^2(\delta_1)+\tan^2(\delta_2)} \tag{19}$$

where δ_1 and δ_2 are functions of the ply stresses. If the applied external load is zero ($\sigma_0 = 0$), Eq. (13) yields $\hat{\sigma}_1 = -\hat{\sigma}_2$, Eq. (18) gives $\delta_1 = \delta_2$, and Eq. (19) reduces to

$$\tan(\delta) = \frac{E}{\eta\omega} + n\frac{\lambda E}{\omega}\hat{\sigma}_1^{\,n-1} \tag{20}$$

Note that Eq. (20) is the same as Eq. (9) except the stress is now the sorption-induced stress in one ply. When there are no sorption-induced stresses, $\hat{\sigma}_1 = \hat{\sigma}_2 = \sigma_0$, Eq. (19) reduces to Eq. (9).

For the case $\sigma_0 = 0$, Eq. (20) predicts that the loss tangent remains elevated above the equilibrium value, $\frac{E}{\eta\omega}$, for as long as the sorption-induced stresses persist. As the magnitude of σ_0 increases, Eq. (19) predicts that the magnitude of the transient loss tangent decreases relative to the equilibrium value given in Eq. (9). For most physically reasonable cases, sorption causes a positive loss tangent transient. However, when a combination of low frequency and large steady load are applied to a material that has high loss, sorption-induced stress concentrations can actually decrease the loss tangent. The general behavior of Eq. (19), with $n=3$, is exhibited in Figure 1 where the loss tangent is normalized to its value with no sorption-induced stresses, Eq. (9), and plotted as a function of the sorption-induced stress imbalance. Curves are given for several values of the nonlinear component of the loss tangent and two values of the linear component of the loss tangent, $\frac{E}{\eta\omega}$. The transient loss tangent is symmetric about $\sigma_1/\sigma_0 = 1$, which corresponds with the case of no stress gradient. When $|\sigma_1 / \sigma_0 - 1| = 1$, the stress is entirely in either the inner or outer plies. For $|\sigma_1 / \sigma_0 - 1| >> 1$, the sorption-induced stresses are greater than the stress created by the applied load and the transient loss tangent is always greater than the steady-state value. For $|\sigma_1 / \sigma_0 - 1|$ on the order of or less than 1, the magnitude of the nonlinear part of the loss tangent with no sorption-induced stresses determines whether the loss tangent increases or decreases upon sorption. The model predicts negative transients (loss tangents below their equilibrium values) for $n\lambda E\hat{\sigma}_0^{\,n-1} / \omega > 0.35$. However, in practice, loss tangents are almost always below 0.35.

As the contribution of the linear response increases compared to the nonlinear contribution to loss tangent, shown for example by comparison of the dashed and solid lines of Figure 1, the relative magnitude of the transient decreases. If the material response were entirely linear, there would be no transient effect in the loss tangent.

NUMERICAL RESULTS

The simple constitutive equation, proposed in Eq. (1), gave us an analytic expression for the transient loss tangent; however, it is not a realistic model for polymers. It evokes the basic transient mechanism, but it misses important response characteristics. The loss tangent from Eq. (1) is inversely proportional to frequency. Actual polymers have multiple thermally activated transitions. Each of these contributes to the loss tangent only when its transition time is of the order of the period of the test load. Thus, as frequency (or temperature) changes, different groups of molecular-level transitions generate losses from sinusoidal loading. These transitions are stress-activated; strain rate increases as the hyperbolic sine of the applied stress [14]. The activation coefficient increases with the amount of motion afforded by the transition. At low frequency, the pertinent transitions require slow, long-range, polymer backbone motions. They accommodate relatively large motions and have large activation coefficients. The high frequency transitions are short, side-chain motions with little movement. The compliances generated by the high frequency transitions therefore can be nearly linear with stress, whereas the low frequency motions are more non-linear. This dependence of load nonlinearity on the time frame of the experiment is manifested in the highly nonlinear response of paper in creep and the relatively linear reaction to standard-speed load-elongation testing.

A representative polymer constitutive equation would have a finite low-load loss tangent that generally decreased with frequency and was more dependent on load at low frequency. To capture these basic features, we made a simple modification to Eq. (1). This was accomplished by adding a Kelvin-Voigt element in series with the terms of Eq. (1). The governing constitutive equation becomes

$$\frac{\partial \varepsilon}{\partial t} = \frac{\partial(\sigma / E)}{\partial t} + \frac{1}{\eta}\sigma + \lambda\sigma^n + \frac{\partial(\beta\Delta m)}{\partial t} + \left[\frac{\partial \tilde{\varepsilon}}{\partial t}\right] \qquad (21)$$

where $\tilde{\varepsilon}$ represents the strain in the Kelvin-Voigt element and

$$\sigma = K\tilde{\varepsilon} + \mu\frac{\partial\tilde{\varepsilon}}{\partial t}. \tag{22}$$

The Kelvin-Voigt element has a relaxation time of μ/K, and it will contribute to the loss tangent for frequencies of the order K/μ. If additional Kelvin-Voigt elements with different relaxation times were added to Eq. (21), a full spectrum of finite loss tangent versus frequency could be obtained. We decided this was unnecessarily tedious, so instead we changed the relaxation time with frequency by prescribing $K/\mu = \omega$. We rationalize this artificial dependence of material properties on experiment as a simple way to get a uniform loss tangent over a wide frequency range. The model now fits our intuition: finite loss tangents at all frequencies with more nonlinearity to load at low frequency. The modified model produced the loss tangent versus frequency and load behavior exhibited in Figure 2. Note that the loss tangent has a finite low-load limit and a nonlinear dependence on load that is pronounced at low frequency. Therefore, loss tangent decays rapidly as a function of frequency only at high loads. The material parameters were taken as

$$\frac{\lambda E^n}{\omega_0} = 10^6,\ \frac{K}{E} = 50,\ \frac{E}{\eta\omega_0} = 10^{-2}, \frac{\omega\mu}{K} = 1,\ \frac{\beta_1}{\beta_2} = 3$$

where ω_0 is a reference frequency with dimensions of radians per unit time.

Next, we numerically subjected the three-ply laminate to the moisture change shown in Figure 3, and a small-amplitude sinusoidal load. Sorption-induced residual stresses are created because of the mismatch in the coefficients of hygroexpansion. The sorption-induced stress in ply 1, which is normalized to the purely elastic sorption-induced stress that would be generated by the same moisture change if there were no viscous flow, is also plotted in Figure 3. Notice that even after moisture equilibrium is reached at a predefined time, $\omega_0 t=15$, residual stresses persist. Over longer times the residual stresses relax away. As shown in the last section, residual stresses lead to transients in the loss tangent.

The loss tangent was determined from a linear perturbation method, and for the case of $\sigma_0 = 0$, it is

$$tan(\delta) = \frac{\left(\frac{E}{\eta\omega} + n\frac{\lambda E}{\omega}\hat{\sigma}_1^{\,n-1}\right)\left(\mu^2\omega^2 + K^2\right) + \mu\omega E}{\mu^2\omega^2 + K^2 + KE}. \tag{23}$$

Figure 4 provides the transient response of the loss tangent, Eq. (22), for three different testing frequencies and the ply-stress history given in Figure 3. The transients persist for as long as residual stresses exist, and as the residual stresses fade, the loss tangent approaches its equilibrium value. The magnitudes of these transients decrease as frequency increases.

SORPTION-INDUCED ARTIFACTS

In the simulation, strains not directly attributable to the sinusoidal loading are removed via the linear perturbation technique. Unfortunately, in physical testing the sinusoidal strain is not so easily separated from hygroexpansive and creep strains. Hygroexpansion during a sinusoidal test cycle produces load-elongation loops that are not closed [4]. These hygroexpansive strains must be removed correctly for the loss tangent determination to be valid. Huge artifacts arise if hygroexpansive strains are not removed at all, and even if they are taken out in a seemingly rational manner, artifacts can remain. This is demonstrated below.

With experimental data, one must determine the loss tangent numerically. For each cycle of the test load, we calculated a loss tangent numerically from the ratio of the first Fourier coefficients of the sinusoidal strain as

$$tan(\delta)\Big|_T = \frac{-\int_{T-\pi/\omega}^{T+\pi/\omega}(\varepsilon-\hat{\varepsilon})cos(\omega t)dt}{\int_{T-\pi/\omega}^{T+\pi/\omega}(\varepsilon-\hat{\varepsilon})sin(\omega t)dt} \qquad (24)$$

where as before $\hat{\varepsilon}$ is the strain determined for the case with no sinusoidal test load, and T is the time at the half cycle of the test load. Eq. (24) agrees with the results of Eqs. (19) and (23) when the average ply stress over a cycle is substituted in the later equations for the ply stress. Assuming that we do not know the extra strain, a first order estimate of $\varepsilon-\hat{\varepsilon}$ is obtained by removing a linear strain component from the total strain based on the initial and final strain of a given cycle. This closes the stress-strain loop in a straightforward manner, but it does not get rid of the artifact for the sorption event of Figure 3. Figure 5 presents loss tangents calculated by this numerical method for a test frequency of $\omega = 5\omega_o$ and two magnitudes of the sinusoidal forcing function. For reference, a no-artifact loss tangent curve is included. Figure 5 demonstrates that large low-frequency loss tangent artifacts can occur during moisture changes and that the artifacts increase as the amplitude of the forcing function decreases. When sorption is complete, the artifact disappears, whereas the transient induced by the stress gradient continues. The artifact is very dependent on the method used to approximate the loss tangent. In a desorption scenario, Eq. (24) with the linear approximation of the extra strain would give negative loss tangents, whereas some other method could give positive loss tangents. As the test frequency increases in relation to the sorption time, there is less hygroexpansive strain in a cycle, and the magnitude of the artifact decreases. The method effectively used by commercial DMTA's is shrouded in details of their loss tangent calculations, and it is beyond our knowledge to comment. Nevertheless, it is extremely likely that large low-frequency artifacts abound.

CONCLUSIONS

We have shown that nonlinear viscoelastic and hygroexpansive materials, such as paper, can exhibit transients in the loss tangent as a result of sorption-induced stresses. We considered transient stresses created during sorption and desorption due to a mismatch in hygroexpansion of plies. Similar stresses would develop if moisture gradients existed during the moisture change or if the mechanical properties of the plies exhibited different dependence on moisture content [11]. No matter how the transient stresses are created, they influence the loss tangent because the compliance is nonlinear in load.

Interpreting DMTA results in a changing humidity environment is a difficult assignment. One must account for temperature changes due to sorption. At low frequencies, hygroexpansive strains occurring during a given cycle greatly influence the loss tangent calculations. These artifacts account for part of the transients and explain to some degree the great disparity of results reported in the literature. Whereas Salmén and Fellers [5] maintain that the loss tangent transient is all an artifact, we propose that part of the effect is real. Improper analysis of the raw data introduces large artifacts, but these last only until sorption is complete.

We selected a constitutive equation that has a known polymer characteristic: nonlinearity in compliance for low frequency and long-time processes. Therefore, as shown in Figure 4, increasing frequency reduced the magnitude of the transient loss tangent. From our perspective, both the non-loop-closure artifact and the real stress-gradient-driven transient fall off at high frequency. This is consistent with the decreases in the loss tangent transient with frequency in DMTA measurements [4,5,8] and with the nonexistence of loss tangent transients at ultrasonic frequencies [9].

ACKNOWLEDGEMENTS

The financial support of the Institute of Paper Science and Technology and its member companies is greatly appreciated.

REFERENCES

1. KUBÁT, J. and LINDBERGSON, B., *J. Appl. Polymer Sci.* 9: 2651-2654 (1965)
2. KUBÁT, J. and LINDBERGSON, B., *Svensk Papperstidn.* 68(21): 743-751 (1965)
3. DE RUVO, A., LUNDBERG, R., MARTIN-LOF, and SOREMARK, C., *The Fundamental Properties of Papers Related to its Uses, Trans. of the Symposium held at Cambridge* 1973, 785-810 (1976)
4. PADANYI, Z. V., *Proceedings of the 1991 International Paper Physics Conference, Kona Hawaii*, 397-411 (1991)
5. SALMÉN, L. and FELLERS, C., *Nordic Pulp and Paper Research Journal* 11(3): 186-191 (1996)
6. JACKSON, T., and PARKER, I., *Proceedings of the 3rd International Moisture and Creep Effects on Paper, Board and Containers*, Rotorua New Zealand, 53-67 (1997)
7. DENIS, E. S., and PARKER, I. H., *Proc. 1995 International Paper Physics Conference*, 143-147 (1995)
8. BERGER, B. J. Doctoral Thesis, The Institute of Paper Chemistry (1988)
9. BERGER, B. J., and HABEGER, C. C., *J. of Pulp and Paper Sci.*, 15(5): J160-J165 (1989)
10. PADANYI, Z. V., in Vol. 1 *Products of Papermaking, Transactions of the Tenth Fundamental Research Symposium*, (Baker, C. F. ed.) Oxford, 521-45 (1993)
11. HABEGER, C. C. and D. W. COFFIN, *J. of Pulp and Paper Sci.*, 26(4): 145-157 (2000)
12. RIEMAN, W. P. and S. H. KURATH, *Tappi J.*, 47(10) 629:633 (1964)
13. RIGDAHL, M. and N. L. SALMÉN, *J. of Mat. Sci.*, 19: 2955-2961 (1984)
14. MEREDITH, E., *Mechanical Properties of Textile Fibers,* New York Interscience Publishers Inc. (1956)

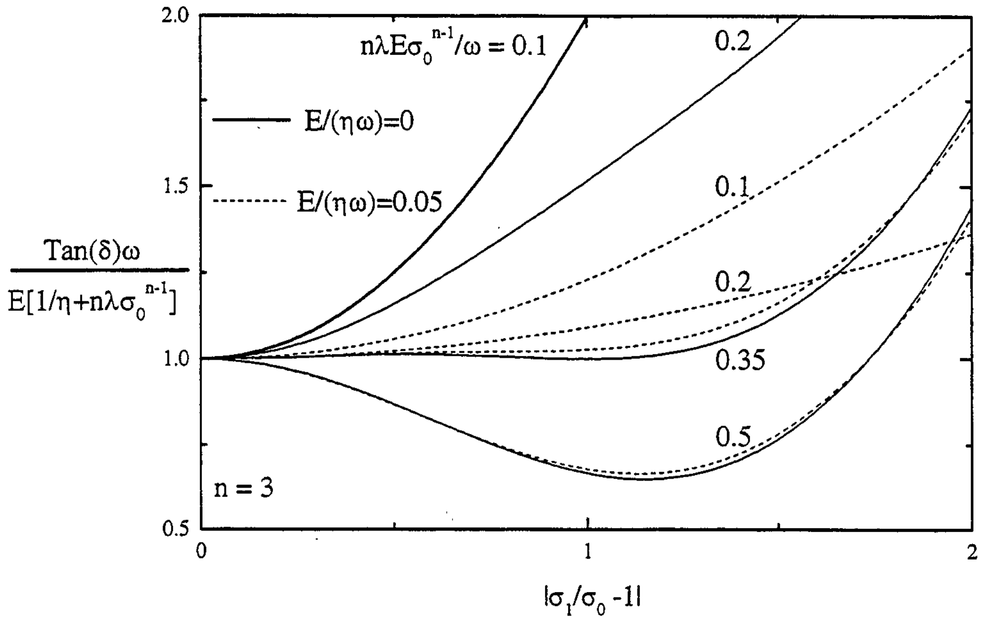

Figure 1. Loss tangent as a function of the distribution of load in a laminate.

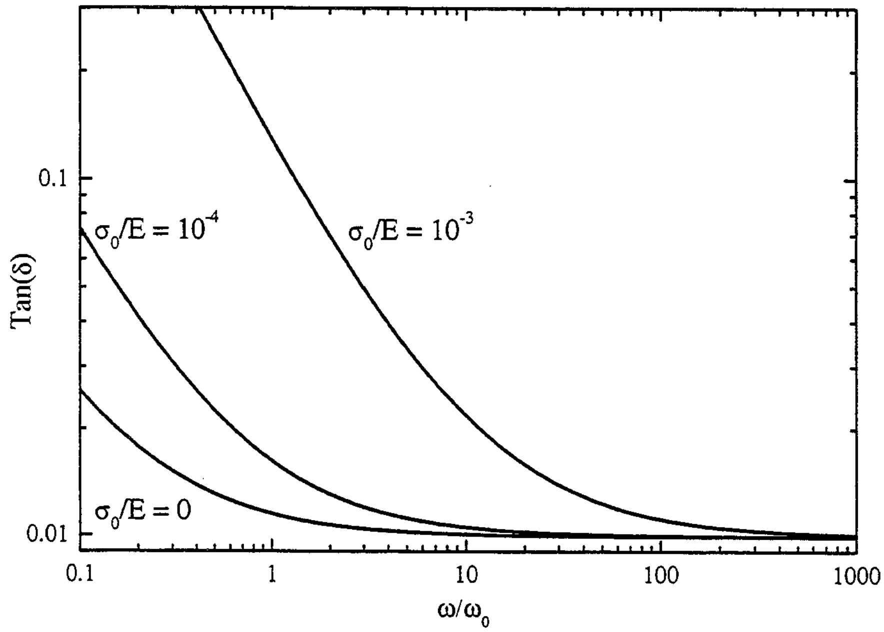

Figure 2. Loss tangent vs. frequency for several magnitudes of load.

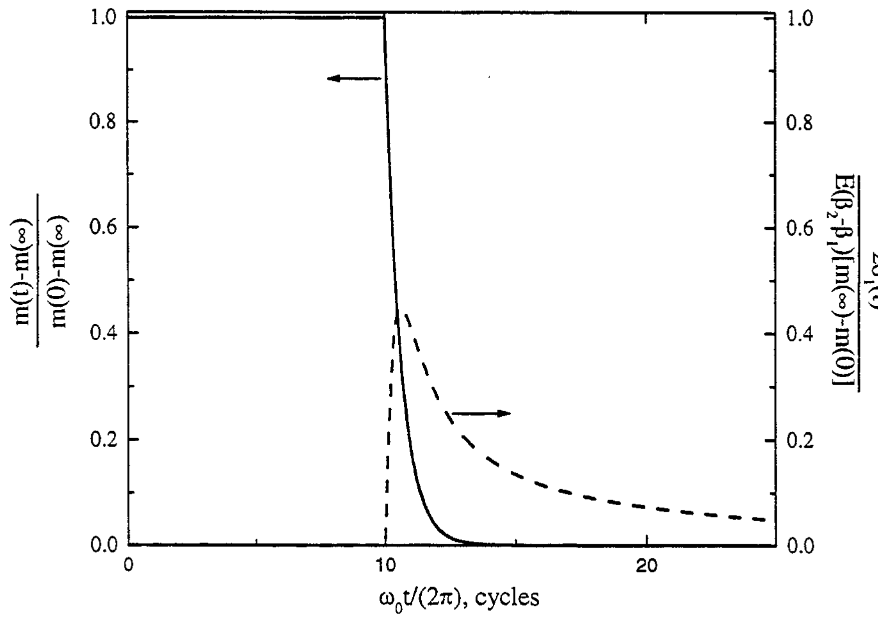

Figure 3. Moisture change and resulting stress in ply-1.

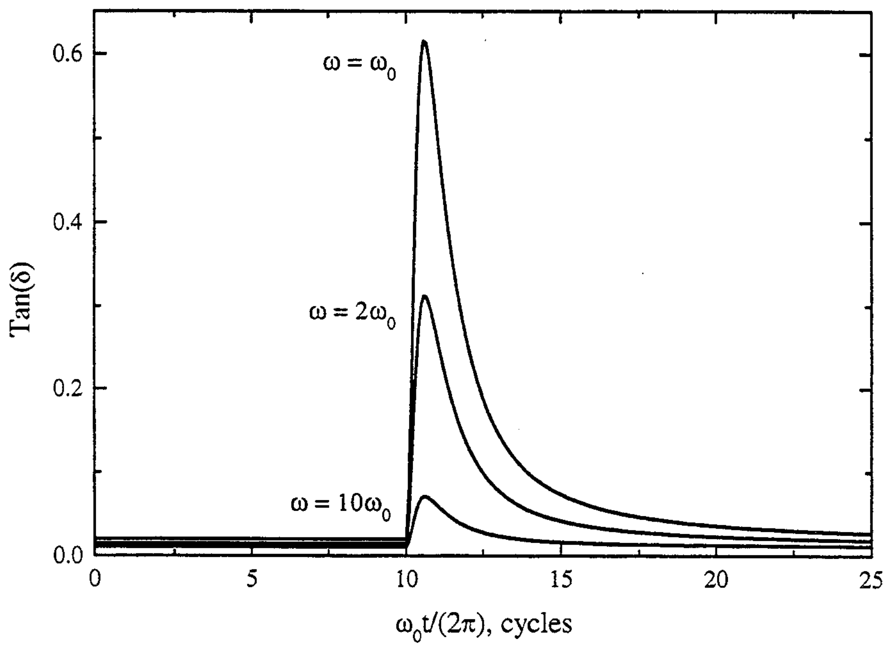

Figure 4. Moisture-induced transients for three frequencies of cyclic load.

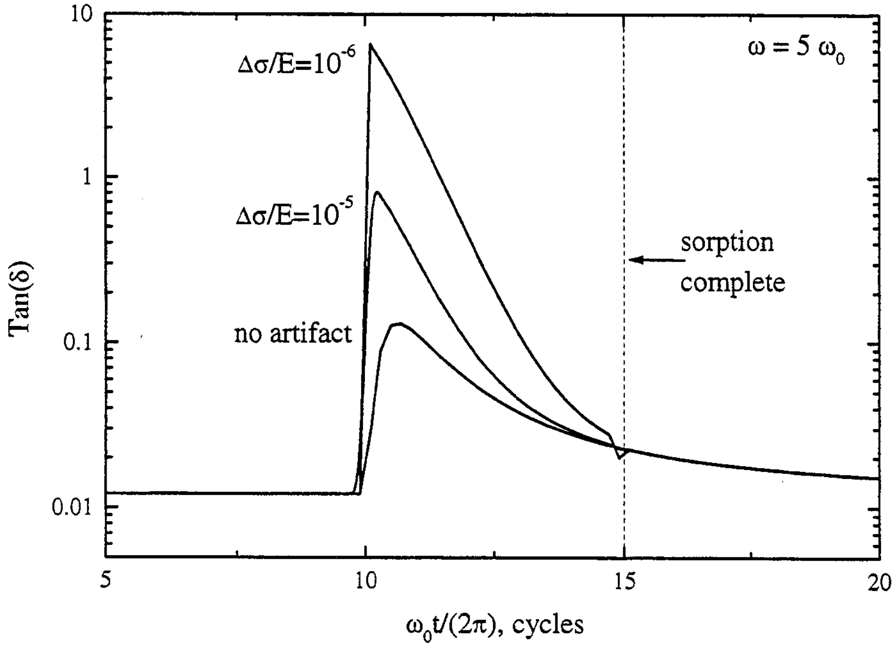

Figure 5. Artifacts in transient loss tangent due to hygroexpansion.